Virology 485 (2015) 322–329

Contents lists available at ScienceDirect

Virology

journal homepage: www.elsevier.com/locate/yviro

Flavivirus sfRNA suppresses antiviral RNA interference in cultured cells and mosquitoes and directly interacts with the RNAi machinery

Stephanie L. Moon, Benjamin J.T. Dodd, Doug E. Brackney [1], Carol J. Wilusz, Gregory D. Ebel, Jeffrey Wilusz *

Department of Microbiology, Immunology and Pathology, Colorado State University, Fort Collins, CO 80523, USA

ARTICLE INFO

Article history:
Received 20 February 2015
Returned to author for revisions
7 August 2015
Accepted 9 August 2015
Available online 29 August 2015

Keywords:
Flavivirus
Dengue virus
Kunjin virus
RNA interference
SfRNA
Mosquito
Arbovirus

ABSTRACT

Productive arbovirus infections require mechanisms to suppress or circumvent the cellular RNA interference (RNAi) pathway, a major antiviral response in mosquitoes. In this study, we demonstrate that two flaviviruses, Dengue virus and Kunjin virus, significantly repress siRNA-mediated RNAi in infected human cells as well as during infection of the mosquito vector *Culex quinquefasciatus*. Arthropod-borne flaviviruses generate a small structured non-coding RNA from the viral 3′ UTR referred to as sfRNA. Analysis of infections with a mutant Kunjin virus that is unable to generate appreciable amounts of the major sfRNA species indicated that RNAi suppression was associated with the generation of the non-coding sfRNA. Co-immunoprecipitation of sfRNA with RNAi mediators Dicer and Ago2 suggest a model for RNAi suppression. Collectively, these data help to establish a clear role for sfRNA in RNAi suppression and adds to the emerging impact of viral long non-coding RNAs in modulating aspects of anti-viral immune processes.

Introduction

RNA interference (RNAi) is a major pathway of antiviral defense in plants and insects (Pumplin and Voinnet, 2013; Kingsolver et al., 2013). The pathway involves the processing of double-stranded RNA (dsRNA) into short 21–22 bp effector RNA molecules by the RNAse III domain-containing Dicer 2 enzyme (Ipsaro and Joshua-Tor, 2015). The fidelity of Dicer cleavage and downstream strand selection in the RNAi process is maintained by Dicer-associated proteins (TRBP and PACT in mammalian cells) (Heyam et al., 2015). These dsRNA serve as targeting moieties when loaded into a RISC complex to selectively downregulate mRNA targets. Argonaute proteins (*e.g.* Ago2) play a major role in the knockdown of gene expression by the RISC complex, mediating selective endonucleolytic cleavage of target RNAs (Dueck and Meister, 2014). The successful avoidance or downregulation of the RNAi machinery is vital for arboviruses to productively infect their arthropod vectors.

Flaviviruses are single-stranded positive-sense RNA viruses that cause a variety of significant human diseases. Many members of this family are arboviruses, using arthropod vectors (primarily mosquitoes) as a key part of their transmission cycles. The Dengue viruses (DENV), West Nile virus (WNV), and Japanese Encephalitis virus (JEV) are examples of flaviviruses with a major impact on human health (Go et al., 2014). The flavivirus genomic RNA contains a single large polyprotein-encoding open reading frame flanked by untranslated regions (UTR). Interestingly, a small subgenomic flavivirus RNA (sfRNA) which represents the 3′ UTR of the viral genomic RNA, is generated not by a subgenomic promoter but rather by stalling of the cellular 5′–3′ exoribonuclease XRN1 as it tries to degrade viral positive-sense transcripts (Pijlman et al., 2008; Funk et al., 2010; Silva et al., 2010; Chapman et al., 2014a, 2014b). Thus in addition to the individual structural and non-structural proteins that are made by the virus, large amounts of this non-coding sfRNA also accumulate in infected cells. The generation of sfRNA has been previously associated with repression of the XRN1 enzyme and stabilization of mRNAs in infected cells (Moon et al., 2012) as well as a sponge for a set of cellular proteins involved in translational regulation of interferon-stimulated mRNAs (Schuessler et al., 2012; Chang et al., 2013; Bidet et al., 2014). Given the increasing appreciation for the major roles played by cellular non-coding transcripts (including regulating the responses to viral infections (Gomez et al., 2013; Ouyang et al., 2014)), it is perhaps not surprising that flaviviruses would also generate a multi-functional non-coding RNA that has a major impact on the outcome of infections.

Many viruses encode RNAi suppressors that down-regulate this arm of the host cell antiviral response and promote efficient viral replication (Szittya and Burgyán, 2013; van Mierlo et al., 2014). Most characterized RNAi suppressors are proteins that bind and

* Corresponding author.
E-mail address: jeffrey.wilusz@colostate.edu (J. Wilusz).
[1] Current address: Department of Environmental Sciences, The Connecticut Agricultural Experiment Station, New Haven, CT 06504, USA.

http://dx.doi.org/10.1016/j.virol.2015.08.009
0042-6822/

sequester dsRNA. Examples of insect virus-encoded RNAi suppressors include the dsRNA binding proteins B2 of flock house virus (Chao et al., 2005), 1A of Drosophila C virus (van Rij et al., 2006), the VP3 proteins of Drosophila X virus and Culex Y virus (van Cleef et al., 2014), and 340R of invertebrate iridescent virus 6 (Bronkhorst et al., 2014). Alternatively, RNAi suppressor proteins can act by directly interacting with RNAi effector proteins. Examples of this strategy in insect viruses include the 1A protein of Cricket paralysis virus (Nayak et al., 2010) and the Vp1 protein of Nora virus (van Mierlo et al., 2012). Both of these proteins bind to the effector protein AGO2 and antagonize its enzymatic activity. Interestingly, the Nora virus Vp1 proteins can show host-specific preferences in AGO2 suppression that may reflect rapid co-evolution of host and viral RNAi-associated factors (van Mierlo et al., 2014). RNA-mediated suppression of RNAi was first documented in cells by analysis of adenoviral VA1 RNA (Lu and Cullen, 2004). Finally, using viral replicons, flavivirus sfRNA has also been implicated as an RNAi suppressor in non-human primate and mosquito cells in culture (Schnettler et al., 2012). However, the biological relevance of these findings during a natural infection, as well as the mechanism of the suppression, are unclear.

In this study we wished to confirm and expand upon observations that sfRNA is an RNAi suppressor (Schnettler et al., 2012). Using viral infections, we demonstrate a mild but statistically significant suppression of siRNA-mediated RNAi in both Dengue virus type 2 (DENV-2) and KUNV infected human cells. Importantly, dsRNA-mediated knockdown of gene expression was also suppressed in live mosquitoes that were infected by KUNV. The suppression of RNAi in KUNV infections in both tissue culture and mosquitoes was dependent on the generation of sfRNA, as a viral variant that fails to generate the major species of sfRNA also failed to suppress RNAi. Finally, we demonstrated a direct interaction between sfRNA sequences and both Dicer and AGO2 host cell proteins, providing important insights into the potential underlying mechanism of RNAi suppression.

Results

Dengue virus type 2 and Kunjin virus infections suppress siRNA-mediated knockdown in human cells

Viral encoded suppressors of RNAi can play a major role during RNA virus infection of plants and insects where RNAi-mediated antiviral defense is a major host response to the accumulation of viral RNAs. Previous work using WNV and DENV-1 replicons has suggested that rather than virally encoded proteins, the sfRNA generated from the 3′ UTR during flavivirus infection serves as a mild suppressor of RNAi in Vero and *Aedes albopictus* U4.4 cells (Schnettler et al., 2012). In order to extend these observations to *bona fide* viral infections, we infected human 293T cells with DENV-2 (Jamaica 1409) and assessed the efficacy of siRNA-directed RNAi. As seen in Fig. 1A, copious amounts of sfRNA was produced at 4 dpi as expected from previous observations (Moon et al., 2012). The major sfRNA species was ~420 nts – and additional minor sfRNA species of shorter size were also observed. This is consistent with previous reports of additional structured regions in the DENV-2 3′ UTR and a small amount of XRN1 exonuclease passing through the 5′-most knot-like structure described previously (Chapman et al., 2014a, 2014b). To assess the relative efficacy of RNAi during DENV-2 infection, mock or DENV-2 infected 293T cells were transfected with an eGFP expressing reporter construct in the presence or absence of an eGFP mRNA-specific siRNA. As seen in Fig. 1B, eGFP mRNA was efficiently expressed in the absence of siRNA in both mock and DENV-2-infected 293T cells. While siRNA to eGFP effectively knocked down

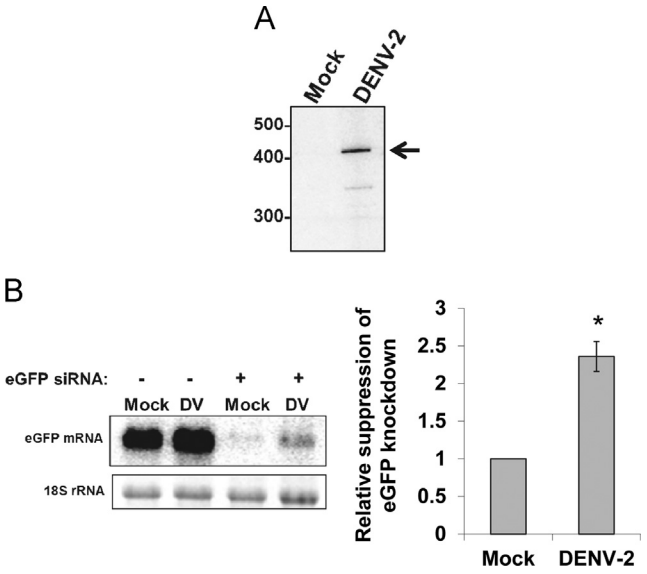

Fig. 1. siRNA-mediated knockdown of a reporter eGFP RNA is suppressed in DENV-2 infected 293T cells. Panel A: A representative northern blot of total RNA from mock infected or DENV-2 infected 293T cells at 4 dpi (MOI of 3) probing for the viral 3′ UTR. The most abundant sfRNA species is denoted by the arrow. Panel B: A representative northern blot to detect the eGFP mRNA in 293T cells transfected with peGFP-N1 with or without an siRNA to the eGFP mRNA at 3 dpi with DENV-2. Total RNA was collected at 4 dpi, residual DNA was removed, and RNA separated on a denaturing agarose gel. The 18S rRNA was visualized by ethidium bromide staining prior to transfer as a loading control. The graph on the right shows quantification of the relative suppression of eGFP siRNA-mediated knockdown in mock infected or DENV-2 infected cells was done by qRT-PCR using primers that spanned the siRNA cleavage site in the eGFP mRNA and *GAPDH* as a reference gene. The *Y* axis reflects the abundance of eGFP mRNA in the cells that received siRNA to eGFP relative to the eGFP abundance in the cells that did not receive siRNA to eGFP. The average ± standard deviation of two independent experiments is shown with * indicating $p < 0.05$ by Student's *t*-test.

eGFP mRNA expression in mock infected cells, siRNA knockdown in DENV-2-infected cells was ~2.5-fold less efficient ($p < 0.05$). *GAPDH* was used as an internal control/reference gene to account for any differences in total mRNA abundance. Note also that the increase in eGFP levels observed in DENV infection (Fig. 1B) was taken into account in deriving siRNA knockdown efficiency by normalizing the eGFP abundances in the DENV infected, siRNA-transfected sample to eGFP abundance in the DENV infected, 'no siRNA' controls. We believe that the reproducibly observed increased levels of eGFP mRNA levels during flavivirus infection are due to XRN1 suppression by sfRNA and subsequent stabilization of cellular mRNAs that we previously reported (Moon et al., 2012). Since sfRNA is present in both siRNA containing and no-siRNA control DENV-2 infected samples, a valid comparison of siRNA knockdown efficiency could be obtained despite the overall increase in eGFP mRNA levels likely due to repression of XRN1-mediated RNA decay. Furthermore, repression of XRN1 activity (using siRNA knockdown) failed to have any effect on the efficiency of siRNAs to target and knock down the eGFP reporter mRNAs (Fig. S1).

These observations were extended to infection of human 293T cells with another flavivirus, KUNV, which also produces sfRNA during infection (Fig. 2A). While eGFP mRNA was effectively knocked down by siRNA transfection in mock-infected cells, siRNA-mediated knockdown of eGFP mRNA expression was ~3-fold less efficient in KUNV-infected cells (Fig. 2B; $p < 0.05$). Importantly, a variant of KUNV containing mutations in the 3′ UTR and cannot generate detectable amounts of the major sfRNA species (Fig. 2A) also failed to effectively suppress RNAi-knockdown of the eGFP reporter mRNA by targeted siRNAs (Fig. 2B) (Pijlman et al., 2008). As performed for DENV-2 infections

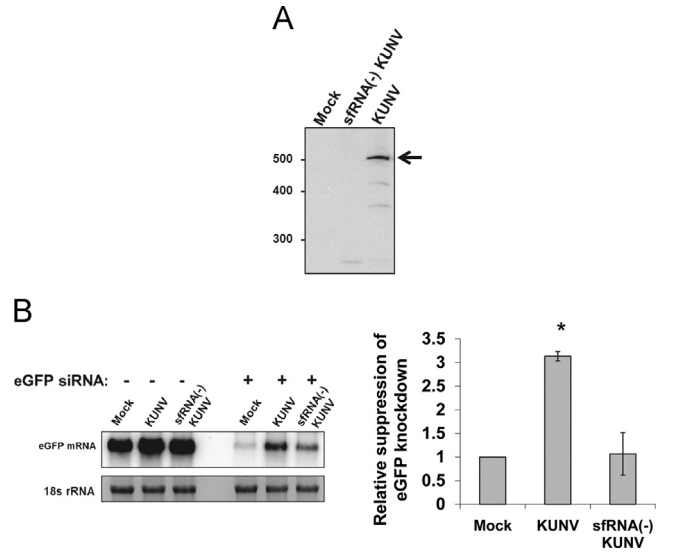

Fig. 2. siRNA-mediated mRNA knockdown is inhibited in KUNV infections in an sfRNA-dependent manner. Panel A: A representative northern blot showing the accumulation of sfRNA at 60 hpi in wild-type KUNV infected 293T cells but not in mock-infected or sfRNA(-) KUNV infected cells. The arrow denotes the most abundant sfRNA species. Panel B: A representative northern blot using purified total RNA from mock infected, wild-type or sfRNA(-) KUNV infected 293T cells at 60 hpi is shown. 293T cells were infected and transfected with peGFP-N1 with or without siRNA to the eGFP mRNA using a probe to the eGFP mRNA. The 18S rRNA detected by ethidium bromide staining was used as a loading control before RNA transfer to nylon membranes. Graph on the right side of the panel: cells were either mock treated or infected with the indicated KUNV isolate and a quantitative assessment of eGFP mRNA abundance in siRNA-treated cells compared to cells transfected with peGFP-N1 alone was done by RT-qPCR using primers that span the eGFP siRNA target site and *GAPDH* as a reference gene. The average of two independent infections is presented with standard deviation and Student's *t*-test depicts significance with * indicating $p < 0.05$.

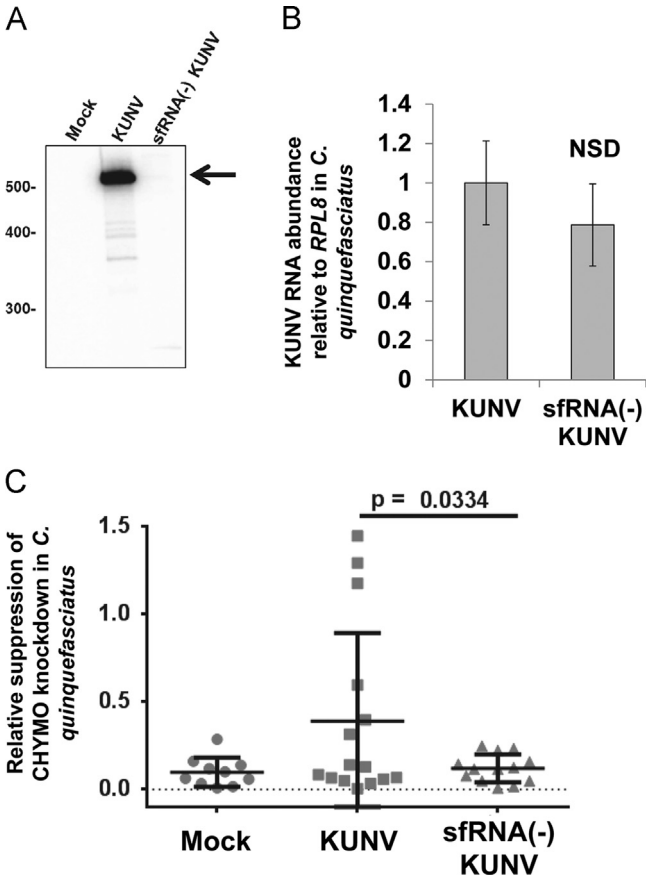

Fig. 3. RNAi activity is suppressed in *Culex quinquefascitus* mosquitoes infected with KUNV in an sfRNA-dependent fashion. Panel A: sfRNA accumulation in mosquitoes infected with wild-type KUNV but not sfRNA(-) KUNV as detected by northern blotting with a probe spanning the viral 3′ UTR. Each lane received 2.5 μg total RNA from pools of 3 or more whole bodies of *C. quinquefasciatus* fed with blood alone or blood containing 1×10^7 PFU/mL of virus, collected at 8 dpi. A representative blot is shown with the arrow indicating the major sfRNA species. Panel B: Relative KUNV RNA abundance in 19 individually collected whole bodies of blood-fed (1×10^7 PFU/mL KUNV or sfRNA(-) KUNV) *C. quinquefasciatus* at 8 dpi determined by RT-qPCR using primers to the viral open reading frame and *RPL8* as a reference gene. The average ± standard deviation is shown with Student's *t*-test used to determine significance (NSD=not significantly different). Panel C: *C. quinquefasciatus* mosquitoes were fed blood alone or 1×10^7 PFU/mL KUNV or sfRNA(-) KUNV and injected with dsRNAs to either a control luciferase mRNA or the endogenous mosquito transcript chymotrypsin (*CHYMO*) 7 days later. At 9 days post-infection (2 days post-injection) mosquitoes were pooled (3 or more per pool), RNA was extracted and analyzed by RT-qPCR for *CHYMO* abundance in mosquitoes that received the *CHYMO* dsRNA relative to mosquitoes that received the luciferase dsRNA using *GADPH* as a reference gene. The above plot depicts results from 3 independent blood feeds/experiments with each gray marker representing relative suppression/inhibition of *CHYMO* mRNA knockdown in a single pool of mosquitoes normalized to luciferase dsRNA injected controls. Statistics were performed using the ROUT method (Q=1%) and *t* tests. The mean is graphed with error bars representing the standard deviation.

described above, *GAPDH* was used as a reference gene to account for small differences in mRNA abundance in each sample. Furthermore, the increase in eGFP levels observed in KUNV infection (Fig. 2B) was taken into account in deriving siRNA knockdown efficiency by normalizing the eGFP abundances in the siRNA-transfected sample to eGFP abundance in 'no siRNA' controls for both mock and KUNV-infected cells. Notably, the sfRNA(-)KUNV variant replicated to similar levels as wild-type KUNV virus in 293T cells as assessed by qRT-PCR analyses of intracellular viral RNA levels (Moon et al., 2012). As stated above, the reproducibly observed increase in the levels of eGFP mRNA during KUNV infection are very likely due to XRN1 suppression by sfRNA and subsequent stabilization of cellular mRNAs that we reported previously (Moon et al., 2012).

Therefore we conclude that RNAi is mildly but significantly suppressed during either DENV-2 or KUNV infection of human cells. Further, consistent with a previous report (Schnettler et al., 2012), the suppression of RNAi is closely associated with sfRNA production. Flaviviral sfRNA was capable of repressing siRNA-mediated RNAi, implying that the small RNA is capable of interfering with the loading of siRNAs into the RISC complex.

KUNV suppresses RNAi in mosquito infection in an sfRNA-dependent fashion

While data from tissue culture infections indicates that flavivirus infections can partially suppress an RNAi response, a key question that remains to be answered is whether a similar effect can be observed during infections of whole mosquitoes. To address this, *Culex quinquefasciatus* mosquitoes were infected with either wild type KUNV or the sfRNA(-)KUNV variant. At 7 dpi, a dramatic accumulation of sfRNA was observed by northern blot of total RNA derived from whole body samples while no sfRNA was observed in total RNA derived from sfRNA-KUNV variant viral infections (Fig. 3A). Importantly, as assayed by RT-qPCR with primers to the viral open reading frame, the amount of viral genomic RNA in these whole body RNA samples did not differ significantly between wild type and sfRNA(-) KUNV infections (Fig. 3B). Thus, as expected, in sfRNA(-) KUNV infections there was a specific defect in the accumulation of the small structured 3′ UTR-derived RNA that was not a result of an overall reduction in viral genomic RNA accumulation.

In order to assess the influence of KUNV sfRNA expression on the efficiency of RNAi activity in infected mosquitoes, dsRNA

against the endogenous mosquito chymotrypsin (*CHYMO*) mRNA was injected and the knockdown of the targeted mRNA was assessed by RT-qPCR analysis relative to control mosquitoes injected with a dsRNA to luciferase. For these analyses, *GAPDH* was used as a reference gene/internal control. As seen in Fig. 3C, expression of the *CHYMO* mRNA was reduced to an average of approximately 10% of control levels in the ten pools of injected uninfected mosquitoes. The efficiency of dsRNA-mediated knockdown of the *CHYMO* mRNA in mosquitoes infected with the sfRNA-KUNV variant was similar to the knockdown efficiency of mock-infected mosquitoes. The dsRNA-mediated knockdown of the *CHYMO* mRNA in wild type KUNV infected mosquitoes, however, was significantly less efficient, reaching an average of only 30% of control levels in the pools of infected mosquitoes that were assayed. Interestingly, the ~3-fold decrease in RNAi efficiency was similar to the levels that were observed in tissue culture. Therefore we conclude that KUNV-infected *C. quinquefasciatus* mosquitoes show a reduced siRNA-mediated RNA response that is dependent upon sfRNA accumulation.

KUNV sfRNA is associated with and may sequester the RNAi mediators Dicer and Ago2

In order to gain insight into a possible mechanism for how sfRNA may partially repress RNAi, we hypothesized that the structured RNA may be capable of interacting with specific RNAi mediators and perhaps sequester and prevent them from functioning effectively in the RNAi pathway. A previous report using recombinant human Dicer protein suggested that sfRNA may specifically target this dsRNA cleaving enzyme (Schnettler et al., 2012). In order to directly assess this, we performed co-immunoprecipitation assays in KUNV infected cells using Dicer antibodies and detected the pull down of any viral RNAs by RT-PCR. As seen in Fig. 4A, the 3′ UTR (and thus presumably sfRNA) was specifically enriched in immunoprecipitations using Dicer antibodies to pulldown Dicer and associated RNAs in KUNV infected 293T cell lysates. Note that formaldehyde was applied to cells to cross-link RNA protein complexes prior to extract preparation and high stringency immunoprecipitation in order to ensure that the complexes being analyzed were likely to represent *bona fide* RNA-protein interactions that occur in infected cells.

The Dicer enzyme, however, is not required for the siRNA-mediated knock down of gene expression that was the focus of this study. Therefore we examined whether KUNV sfRNA was capable of directly interacting with a dsRNA-binding RISC complex component (Takahashi et al., 2014). As seen in Fig. 4B, the 3′ UTR (and thus presumably sfRNA) was specifically enriched in immunoprecipitations using AGO2 antibodies to pull down this key RISC component and associated RNAs in cross-linked KUNV infected 293T cell lysates. Fig. 4C demonstrates that the co-immunoprecipitation of the 3′ UTR portion of KUNV was significant, as another RNA binding protein (CUGBP1 or CELF1) failed to immunoprecipitate viral transcripts above the background level of the IgG control.

In summary, we conclude that the highly structured sfRNA is capable of interacting with the RNAi effectors Dicer and AGO2 in infected cells. This may provide a mechanistic explanation for the suppression of RNAi activity observed in DENV-2 and KUNV infections.

Discussion

The data presented above represent three important observations regarding the interface between the cellular RNAi pathway and flaviviruses. First, we demonstrated that siRNA-mediated RNAi knockdowns in human cells could be suppressed by flavivirus infection in an sfRNA-dependent fashion. These data build upon previously published observations (Schnettler et al., 2012), extending RNAi suppression by sfRNA to the context of a flaviviral infection. Second, data presented in Fig. 3 above extend sfRNA-mediated RNAi suppression by KUNV to the context of a *C. quinquefasciatus* mosquito infection. This is an important demonstration of the phenomenon in the context of an arthropod vector and is a key step towards establishing the biological relevance of sfRNA-mediated RNAi suppression. Finally, data in Fig. 4 suggest that an important aspect of the suppression of RNAi by flaviviruses may be the interaction between sfRNA and two key RNAi mediators – Dicer and AGO2. Collectively, these observations provide a clearer picture of RNAi suppression by flaviviruses and present several implications with significant impact to flavivirus biology.

Based on the interaction of sfRNA with Dicer and AGO2 that was revealed by co-immunoprecipitation from infected cell extracts, we propose a model for sfRNA-mediated RNAi suppression depicted in Fig. 5. The generation of large amounts of sfRNA by the XRN1 exoribonuclease stalling at the knot-like structures at the proximal (5′) side of the 3′ UTR (Chapman et al., 2014a) allows

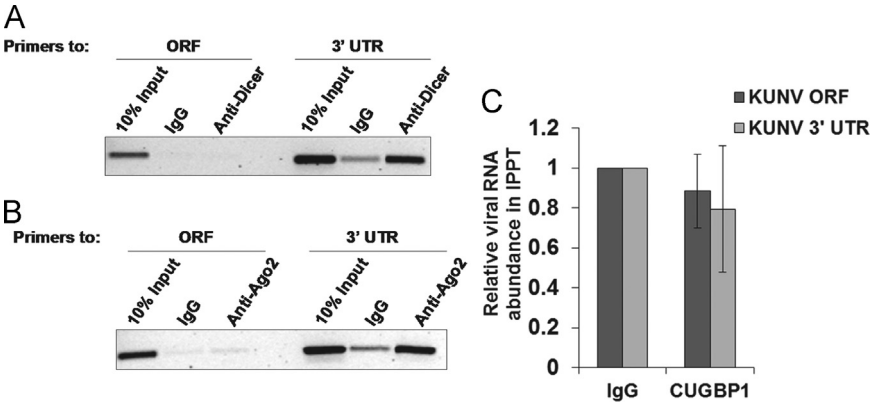

Fig. 4. Kunjin virus 3′ UTR RNAs are associated with Dicer and Ago2 proteins by co-immunoprecipitation analysis. Antibodies to RNA induced silencing complex components Dicer (Panel A) or AGO2 (Panel B) were used to co-purify RNA from wild-type KUNV infected 293T cells (60 hpi, MOI of 5) following formaldehyde cross-linking to stabilize complexes *in vivo*. Normal rabbit or rat IgG antibodies were used as non-specific controls. Isolated RNAs were amplified by RT-PCR using primers to the KUNV open reading frame upstream of the sfRNA start site (ORF) or to the viral 3′ untranslated region (3′ UTR) and PCR products were visualized on agarose gels by ethidium bromide staining. Representative gels are shown. Panel C: Formaldehyde cross-linked lysates from Kunjin virus infected 293T cells (60 h post-infection) were subjected to RNA-protein co-immunoprecipitation using CUGBP1 antibody or a control normal rabbit IgG. Co-purifying RNAs and RNAs from 10% input samples were reverse transcribed and qPCR performed using primers to the Kunjin virus open reading frame ("KUNV ORF") or 3′ UTR ("KUNV 3′ UTR"). The abundance of each KUNV RNA was determined relative to the 10% input and normal IgG control. The average ± standard deviation from three independent infections is shown.

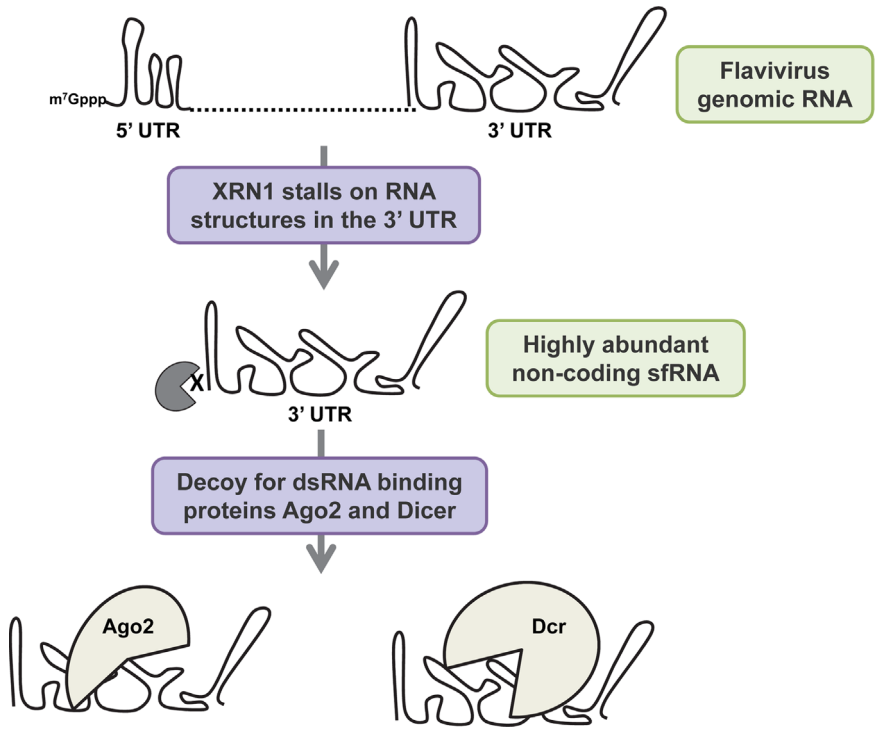

Fig. 5. Model depicting formation of sfRNA and the function of the non-coding transcript in RNAi suppression. The cellular exonuclease XRN1 generates large amounts of non-coding sfRNA by partial decay of the flavivirus genomic RNA. The accumulation of sfRNA permits sequestration of dsRNA binding proteins Dicer and AGO2, leading to a mild suppression of the RNAi machinery in human and mosquito cells.

for sufficient RNA substrate for the binding and temporary sequestration of Dicer and AGO2 – two of the main RNAi enzymatic proteins with dsRNA binding domains. The extensive folding and dsRNA-like properties of sfRNA likely play a key role in interacting with these enzymes. Consistent with this, previous attempts at mapping the requisite regions of sfRNA required for RNAi suppression demonstrated that regions beyond the extended 3′ most stem loop structure were important and sufficient for suppression (Schnettler et al., 2012). One possible explanation for the partial repression of RNAi despite the binding of two important RNAi mediators by sfRNA is that the RNA-protein interaction may have a relatively quick dissociation rate, thus resulting in only a temporary suppression. The large amount of sfRNA produced in the infected cell would provide a substantial pool of reversible inhibitor, thus providing for additional sfRNA molecules to bind when another is released, resulting in a significant but by no means complete inhibition of the RNAi process. A second model for partial RNAi suppression by sfRNA could be a relatively low or variable affinity of sfRNA for Dicer and AGO2 depending on the organism. Differences in binding site topology between different AGO2 proteins from different species (Kandeel and Kitade, 2013) could also play an interesting role in sfRNA-mediated repression. Furthermore, given that RNAi genes are among the fastest evolving genes in mosquitoes (Bernhardt et al., 2012), one could even speculate that differences in AGO2 binding site topology may potentially play a role in vector competence in some instances.

While conventional models present RNAi as a 'black and white' cellular defense mechanism in the arms race between flaviviruses and the mosquito, adding a little bit of 'gray' to this model may be biologically very relevant. A three-fold decrease in mosquito RNAi efficiency in a flavivirus infected cell may not seem extremely impressive at first glance, but one must keep in mind arboviruses must not only replicate to high levels in the mosquito vector but also minimize mosquito pathology in order to insure completion of the infection/transmission cycle. Transient silencing of genes in the RNAi pathway has been shown to increase the replication of DENV-2 and allow the virus to better overcome midgut escape barriers (Khoo et al., 2013). However the inclusion of a very effective RNAi inhibitor (*e.g.* the Flockhouse virus B2 protein) has also been associated with significantly higher mosquito vector mortality (Myles et al., 2008; Cirimotich et al., 2009). Thus a partial repression of RNAi that balances both the needs of the arbovirus as well as minimizes the pathological effects on the mosquito host may be an important key to the ultimate success in the flavivirus transmission cycle.

The sfRNA that is generated from the 3′ UTR of all arthropod-associated flaviviruses is emerging as an interesting multifunctional non-coding RNA (Roby et al., 2014). In addition to its ability to suppress RNAi outlined in this study, the small RNA has two other impacts on the host cell. First, the generation of sfRNA by XRN1 represses the activity of this exoribonuclease that plays a major role in cellular mRNA decay (Jones et al., 2012; Moon et al., 2012). This repression appears to feedback and shut down the entire 5′–3′ mRNA decay pathway, resulting in the stabilization of cellular mRNAs (Moon et al., 2012, 2015). This causes a major dysregulation of cellular gene expression that may influence cytopathology and have implications to viral pathogenesis (Pijlman et al., 2008). The repression of XRN1 by sfRNA (Moon et al., 2012) also accounted for the reproducible increased overall eGFP levels compared to mock infected cells or cells infected with a KUNV variant that was unable to produce sfRNA (Figs. 1 and 2). Second, sfRNA serves as a binding site for several important cellular proteins, including G3BP1, G3BP2 and CAPRIN that are required for the efficient translation of several interferon-induced mRNAs (Bidet et al., 2014). Thus, although the overall significance of RNAi to antiviral activity in mammalian cells is currently under debate (Cullen et al., 2013), sfRNA may still reduce mammalian antiviral responses by dysregulating aspects of the interferon pathway. Interestingly, flaviviruses may not be alone among arboviruses in having distinct roles for their 3′ UTRs in mammalian

versus mosquito cells. Recently the alphavirus Sindbis virus was shown to maintain miRNA target sites in its 3′ UTR which restrict growth in dendritic cells to downgrade the overall mammalian antiviral response and use this same region in mosquito cells to maintain efficient replication by a yet to be described mechanism (Trobaugh et al., 2014).

There are numerous questions remaining for future studies regarding the role of sfRNA in suppressing RNAi. It will be interesting, for example, to demonstrate the biological importance and evolutionary impact for the alleged need for partial RNAi repression in flavivirus biology. It will also be interesting to map the sequences/structures required for RNAi suppression and to determine whether and how sfRNA interacts with other less well understood RNAi pathways (*e.g.* piRNA, *etc.*). These structures could represent targets for antiviral therapeutics or perhaps interesting genomic regions to manipulate to create attenuated viruses for vaccine development. The foundation provided by this study will hopefully fuel additional effort in this area.

Material and methods

Viruses and cells

Human 293T cells were cultured in Dulbecco's Minimal Essential Medium (DMEM; Mediatech) with 10% fetal bovine serum (Atlas Biologicals) and 1% streptomycin/penicillin (Fisher Scientific-Hyclone). Dengue virus type 2 (Jamaica 1409; GenBank: M20558.1) was amplified on *A. albopictus* C6/36 mosquito cells and titered on LLC-MK2 cells. Kunjin virus (FLSDX; Genbank: AY274504.1) and the sfRNA-deficient Kunjin virus (FLSDX IRAΔCS3 described in Pijlman et al. (2008)) were amplified and titered on Vero or BHK-21 cells. 293T cells were infected with DENV-2 (MOI of 3), KUNV (MOI of 10), or sfRNA(-) KUNV (MOI of 10) by allowing virus to adsorb for 2 h at which time cells were washed twice with warm DMEM to remove residual viral particles.

siRNA knockdown in 293T cells

All plasmids were purified using PureLink® HiPure plasmid maxiprep kit (Life Technologies) and treated with the MiraCLEAN® endotoxin removal kit (Mirus) prior to transfection. Twenty four hours prior to RNA collection, infected or mock infected 293T cells were transfected with peGFP-N1 and a duplex siRNA to eGFP (5′-GCAAGCUGACCCUGAAGUUCAU) or an equal volume of water using Lipofectamine® 2000 (Life Technologies) according to the manufacturer's protocol. Total RNA from mock infected, KUNV or sfRNA(-) KUNV infected cells was collected at 60 h post-infection and RNA from DENV-2 infections was collected at 4 days post-infection using TRIzol® (Life Technologies).

Mosquito infections and injections: in vivo RNAi inhibition assay

Intrathoracic inoculation of long double stranded RNA (dsRNA) is a commonly used approach for silencing endogenous genes within mosquitoes and has been used to effectively silence numerous midgut specific protease genes (Brackney et al., 2008). Therefore, using this method, we were able to examine the potential RNAi inhibitory effects of a flavivirus sfRNA *in vivo*. Briefly, adult female *C. quinquefasciatus* mosquitoes were offered a bloodmeal containing 1×10^7 PFU/mL of KUNV or sfRNA(-) KUNV 3–4 days post-eclosion. Engorged females were collected and housed at 27 °C with a 14:10 light:dark cycle in order to allow midgut infections to become established. During this time female mosquitoes were allowed to deposit their eggs in egg-laying cups. The generation of chymotrypsin dsRNA has been previously described (Brackney et al., 2008). Briefly, DNA templates were generated for *C. quinquefasciatus CHYMO* using the following primers: T7 *CHYMO* Fw 5′-TAATACGACTCACTATAGGGGCTGCCCACTGCGAAACCGAGTA and T7 *CHYMO* Rv 5′-TAATACGACTCACTATAGGGCAGGACACGACTCCGACCTGAAC. Seven days post-infection, mosquitoes were intrathoracically inoculated with 210 ng of dsRNA specific for chymotrypsin or a non-specific control dsRNA against luciferase. Following a two day incubation, whole mosquitoes were collected, pooled, homogenized in TRIzol reagent and RNA extracted according to the manufacturer's instructions (Invitrogen). Total RNA was Turbo DNAse treated (Life Technologies) according to manufacturer's protocol followed by phenol/chloroform extraction. Reverse transcriptions using random hexamers were preformed according to manufacturer's protocol (Superscript III First Strand Synthesis System, Invitrogen) with 500 ng of total input RNA. qPCR was performed as described below (iQ Syber Green Supermix) using *GAPDH* as a reference gene. Chymotrypsin dsRNA injected samples were normalized to negative control Luciferase dsRNA samples. *C. quinquefasciatus* qPCR primers were as follows: *CHYMO* Fw 5′-CAACATGGCATCGAAACTGAC; *CHYMO* Rv 5′-GCTCCACAAAAGTGCAACG; *GAPDH* Fw 5′-TCAAGCAGAAGGTCAAGGAAG; *GAPDH* Rv 5′-GTTGTCGTACCAGGAGATGAG.

RNA analyses

RNA probes for detection of eGFP mRNA, DENV-2 sfRNA or KUNV sfRNA were generated by internally radiolabeled T7 *in vitro* transcriptions using linearized pGEM4 plasmid templates harboring the full-length 3′ UTR of KUNV (FLSDX) or DENV-2 (Jamaica 1409) in the EcoRI and HindIII sites described in Moon et al. (2012). The 782 nt eGFP open reading frame was subcloned from peGFP-N1 into the multiple cloning site of pGEM-4 by digestion with EcoRI and XbaI. Northern blotting to detect sfRNA from infected 293T cells transfected with eGFP was done by separating total RNA on formaldehyde agarose gels, transfer to a nylon membrane and probing for the eGFP open reading frame. An image of ethidium bromide staining of the 18S rRNA was taken prior to transfer as a loading control. A representative northern blot from two independent infections is shown. For sfRNA detection in infected *C. quinquefasciatus*, 2.5 μg total RNA isolated from pools of 5 mosquitoes injected with a control dsRNA to luciferase at 8 dpi with KUNV, sfRNA(-) KUNV, or blood-fed only was separated on a 5% polyacrylamide gel, transferred to nylon membrane, and probed with the radiolabeled antisense 3′ UTR RNA of KUNV. A representative northern blot out of three independently collected pools of mosquitoes is shown.

To assess eGFP knockdown in 293T cells, isolated RNA from 293T cells was treated with DpnI and EcoRI (New England Biolabs) to linearize any remaining peGFP-N1 plasmid in the presence of RiboLock RNase Inibitor (Thermo Scientific) for 1 h at 37 °C. Residual genomic or plasmid DNA was removed by TURBO™ DNase (Life Technologies) treatment at 37 °C for 30 min. Reverse transcriptions were performed with 1 μg RNA from each sample using the Improm-II™ system (Promega) and random hexamers according to the manufacturer's instructions. Resulting cDNA was diluted 1:200 for qPCR detection of eGFP using primers that spanned the siRNA target site (eGFP Fw: 5′-GACGGCGACGTAAACGGCCA; eGFP Rv: 5′-CAGCTTGCCGGTGGTGCAGA) and *GAPDH* was used as a reference gene (*GAPDH* Fw: 5′-TCTTTTGCGTCGCCAGCCGA; *GAPDH*; Rv: 5′-ACCAGGCGCCCAATACGACC). qPCR was performed using a CFX96 Real Time PCR Detection system (Bio Rad) and iQ™ SYBR® Green Supermix (Bio Rad). All qPCR primers had efficiencies between 90 and 110%. The abundance of eGFP mRNA in each sample was determined using the ΔΔCt method, and the relative suppression of eGFP knockdown was calculated by normalizing eGFP expression in peGFP-N1 + siRNA transfected samples to peGFP-N1 + water transfected samples.

The average ± standard deviation of the fold repression in eGFP knockdown for each condition (mock, DENV-2, KUNV, or sfRNA(-) KUNV) from two independent infections is reported. Significance was determined using Student's *t*-test.

The abundance of KUNV RNA in wild-type and sfRNA(-) KUNV infections in *C. quinquefasciatus* was assessed by RT-qPCR relative to the endogenous *RPL8* transcript. Reverse transcriptions were done as described above using random hexamers and ~250 ng of total RNA from 19 individual mosquitoes collected at 8 days post-feeding on blood containing 1×10^7 PFU/mL of either wild-type or sfRNA(-) KUNV. The following primers were used for qPCR: *RPL8* Fw: 5′-CATCCGTGCACAGCGTAAAG; *RPL8* Rv: 5′-GTGCTTCAC-GACTCCCTTCA; KUNV ORF Fw: 5′-TGGACGGGGAATACCGACTTA-GAGG; KUNV ORF Rv: 5′-ACCCCAGCTGCTGCCACCTT. The average KUNV RNA abundance ± standard deviation is reported with significance assessed by *t*-test.

RNA co-immunoprecipitation and analyses

Briefly, 293T cells were infected with KUNV (MOI of 5) and RNA-protein complexes were stabilized by formaldehyde cross-linking at 60 h post-infection. Immunoprecipitations were done using rabbit anti-Dicer (Santa Cruz Biotechnology; H-212), rat anti-Ago2 (Millipore; 11A9), CUGBP-1 (3B1; Santa Cruz Biotechnology) or an equal quantity of normal rabbit IgG (Santa Cruz Biotechnology) or normal rat IgG (Santa Cruz Biotechnology). Equal volumes of RNA isolated from the 10% input, IgG control, Dicer, or Ago2 immunoprecipitated samples were reverse transcribed with random hexamer primers as described above. The KUNV ORF or 3′ UTR was detected by semi-quantitative PCR and agarose gel electrophoresis or real-time qPCR using the primers list above to the KUNV ORF or the following: KUNV 3′ UTR Fw: 5′-GGAGACCCCGTGCCGCAAAA; KUNV 3′ UTR Rv: 5′-CACTGTGCCGTGTGGCTGGT. Agarose gels were stained with ethidium bromide and imaged using Image Lab™ Software (Bio-Rad). Results were confirmed using RNA from an independent infection by qPCR with a representative agarose gel presented.

Acknowledgments

We wish to thank Wahida Khan for assistance with aspects of the project and members of the Wilusz laboratory for helpful comments. We also thank Nathan Grubaugh for assistance with mosquito collection and Alexander Khromykh for the FLSDX KUNV clone. These studies were supported by an NIAID award through the Rocky Mountain Regional Center of Excellence (U54 AI-065357) to J.W. SLM received support from a USDA NIFA NNF training grant (2010-38420-20367). Portions of this work were funded by a grant from the National Institute of Allergy and Infectious Disease, National Institutes of Health under grant number AI067380 (GDE).

Appendix A. Supporting information

Supplementary data associated with this article can be found in the online version at http://dx.doi.org/10.1016/j.virol.2015.08.009.

References

Bernhardt, S.A., Simmons, M.P., Olson, K.E., Beaty, B.J., Blair, C.D., Black, W.C., 2012. Rapid intraspecific evolution of miRNA and siRNA genes in the mosquito *Aedes aegypti*. PLoS One 7 (9), e44198. http://dx.doi.org/10.1371/journal.pone.0044198.

Bidet, K., Dadlani, D., Garcia-Blanco, M.A., 2014. G3BP1, G3BP2 and CAPRIN1 are required for translation of interferon stimulated mRNAs and are targeted by a dengue virus non-coding RNA. PLoS Pathog. 10 (7), e1004242.

Brackney, D.E., Foy, B.D., Olson, K.E., 2008. The effects of midgut serine proteases on dengue virus type 2 infectivity of *Aedes aegypti*. Am. J. Trop. Med. Hyg. 79 (2), 267–274.

Bronkhorst, A.W., van Cleef, K.W., Venselaar, H., van Rij, R.P., 2014. A dsRNA-binding protein of a complex invertebrate DNA virus suppresses the Drosophila RNAi response. Nucleic Acids Res. 42 (19), 12237–12248.

Chao, J.A., Lee, J.H., Chapados, B.R., Debler, E.W., Schneemann, A., Williamson, J.R., 2005. Dual modes of RNA-silencing suppression by Flock House virus protein B2. Nat. Struct. Mol. Biol. 12 (11), 952–957.

Chapman, E.G., Costantino, D.A., Rabe, J.L., Moon, S.L., Wilusz, J., Nix, J.C., Kieft, J.S., 2014a. The structural basis of pathogenic subgenomic flavivirus RNA (sfRNA) production. Science 344 (6181), 307–310.

Chapman, E.G., Moon, S.L., Wilusz, J., Kieft, J.S., 2014b. RNA structures that resist degradation by Xrn1 produce a pathogenic dengue virus RNA. Elife 3, e01892. http://dx.doi.org/10.7554/eLife.01892.

Chang, R.Y., Hsu, T.W., Chen, Y.L., Liu, S.F., Tsai, Y.J., Lin, Y.T., Chen, Y.S., Fan, Y.H., 2013. Japanese encephalitis virus non-coding RNA inhibits activation of interferon by blocking nuclear translocation of interferon regulatory factor 3. Vet. Microbiol. 166 (1-2), 11–21.

Cirimotich, C.M., Scott, J.C., Phillips, A.T., Geiss, B.J., Olson, K.E., 2009. Suppression of RNA interference increases alphavirus replication and virus-associated mortality in *Aedes aegypti* mosquitoes. BMC Microbiol. 9, 49. http://dx.doi.org/10.1186/1471-2180-9-49.

Cullen, B.R., Cherry, S., tenOever, B.R., 2013. Is RNA interference a physiologically relevant innate antiviral immune response in mammals? Cell Host Microbe 14 (4), 374–378.

Dueck, A., Meister, G., 2014. Assembly and function of small RNA – argonaute protein complexes. Biol. Chem. 395 (6), 611–629.

Funk, A., Truong, K., Nagasaki, T., Torres, S., Floden, N., Balmori Melian, E., Edmonds, J., Dong, H., Shi, P.Y., Khromykh, A.A., 2010. RNA structures required for production of subgenomic flavivirus RNA. J. Virol. 84 (21), 11407–11417.

Go, Y.Y., Balasuriya, U.B., Lee, C.K., 2014. Zoonotic encephalitides caused by arboviruses: transmission and epidemiology of alphaviruses and flaviviruses. Clin. Exp. Vaccine Res. 3 (1), 58–77.

Gomez, J.A., Wapinski, O.L., Yang, Y.W., Bureau, J.F., Gopinath, S., Monack, D.M., Chang, H.Y., Brahic, M., Kirkegaard, K., 2013. The NeST long ncRNA controls microbial susceptibility and epigenetic activation of the interferon-γ locus. Cell 152 (4), 743–754.

Heyam, A., Lagos, D., Plevin, M., 2015. Dissecting the roles of TRBP and PACT in double-stranded RNA recognition and processing of noncoding RNAs. Wiley Interdiscip. Rev.: RNA 6, 271–289. http://dx.doi.org/10.1002/wrna.1272.

Ipsaro, J.J., Joshua-Tor, L., 2015. From guide to target: molecular insights into eukaryotic RNA-interference machinery. Nat. Struct. Mol. Biol. 22 (1), 20–28.

Jones, C.I., Zabolotskaya, M.V., Newbury, S.F., 2012. The 5′→3′ exoribonuclease XRN1/Pacman and its functions in cellular processes and development. Wiley Interdiscip. Rev.: RNA 3 (4), 455–468.

Kandeel, M., Kitade, Y., 2013. In silico molecular docking analysis of the human Argonaute 2 PAZ domain reveals insights into RNA interference. J. Comput. Aided Mol. Des. 27 (7), 605–614.

Khoo, C.C., Doty, J.B., Heersink, M.S., Olson, K.E., Franz, A.W., 2013. Transgene-mediated suppression of the RNA interference pathway in *Aedes aegypti* interferes with gene silencing and enhances Sindbis virus and dengue virus type 2 replication. Insect Mol. Biol. 22 (1), 104–114.

Kingsolver, M.B., Huang, Z., Hardy, R.W., 2013. Insect antiviral innate immunity: pathways, effectors, and connections. J. Mol. Biol. 425 (24), 4921–4936.

Lu, S., Cullen, B.R., 2004. Adenovirus VA1 noncoding RNA can inhibit small interfering RNA and MicroRNA biogenesis. J. Virol. 78 (23), 12868–12876.

Moon, S.L., Anderson, J.R., Kumagai, Y., Wilusz, C.J., Akira, S., Khromykh, A.A., Wilusz, J., 2012. A noncoding RNA produced by arthropod-borne flaviviruses inhibits the cellular exoribonuclease XRN1 and alters host mRNA stability. RNA 18 (11), 2029–2040.

Moon, S.L., Blackinton, J.G., Anderson, J.R., Dozier, M.K., Dodd, B.J., Keene, J.D., Wilusz, C.J., Bradrick, S.S., Wilusz, J., 2015. XRN1 stalling in the 5′ UTR of hepatitis C virus and bovine viral diarrhea virus is associated with dysregulated host mRNA stability. PLoS Pathog. 11 (3), e1004708.

Myles, K.M., Wiley, M.R., Morazzani, E.M., Adelman, Z.N., 2008. Alphavirus-derived small RNAs modulate pathogenesis in disease vector mosquitoes. Proc. Natl. Acad. Sci. USA 105 (50), 19938–19943.

Nayak, A., Berry, B., Tassetto, M., Kunitomi, M., Acevedo, A., Deng, C., Krutchinsky, A., Gross, J., Antoniewski, C., Andino, R., 2010. Cricket paralysis virus antagonizes Argonaute 2 to modulate antiviral defense in Drosophila. Nat. Struct. Mol. Biol. 17 (5), 547–554.

Ouyang, J., Zhu, X., Chen, Y., Wei, H., Chen, Q., Chi, X., Qi, B., Zhang, L., Zhao, Y., Gao, G.F., Wang, G., Chen, J.L., 2014. NRAV a long noncoding RNA, modulates antiviral responses through suppression of interferon-stimulated gene transcription. Cell Host Microbe 16 (5), 616–626.

Pijlman, G.P., Funk, A., Kondratieva, N., Leung, J., Torres, S., van der Aa, L., Liu, W.J., Palmenberg, A.C., Shi, P.Y., Hall, R.A., Khromykh, A.A., 2008. A highly structured, nuclease-resistant, noncoding RNA produced by flaviviruses is required for pathogenicity. Cell Host Microbe 4 (6), 579–591.

Pumplin, N., Voinnet, O., 2013. RNA silencing suppression by plant pathogens: defence, counter-defence and counter-counter-defence. Nat. Rev. Microbiol. 11 (11), 745–760.

Roby, J.A., Pijlman, G.P., Wilusz, J., Khromykh, A.A., 2014. Noncoding subgenomic flavivirus RNA: multiple functions in West Nile virus pathogenesis and modulation of host responses. Viruses 6 (2), 404–427.

Schnettler, E., Sterken, M.G., Leung, J.Y., Metz, S.W., Geertsema, C., Goldbach, R.W., Vlak, J.M., Kohl, A., Khromykh, A.A., Pijlman, G.P., 2012. Noncoding flavivirus RNA displays RNA interference suppressor activity in insect and mammalian cells. J. Virol. 86 (24), 13486–13500.

Schuessler, A., Funk, A., Lazear, H.M., Cooper, D.A., Torres, S., Daffis, S., Jha, B.K., Kumagai, Y., Takeuchi, O., Hertzog, P., Silverman, R., Akira, S., Barton, D.J., Diamond, M.S., Khromykh, A.A., 2012. West Nile virus noncoding subgenomic RNA contributes to viral evasion of the type I interferon-mediated antiviral response. J. Virol. 86 (10), 5708–5718.

Silva, P.A., Pereira, C.F., Dalebout, T.J., Spaan, W.J., Bredenbeek, P.J., 2010. An RNA pseudoknot is required for production of yellow fever virus subgenomic RNA by the host nuclease XRN1. J. Virol. 84 (21), 11395–11406.

Szittya, G., Burgyán, J., 2013. RNA interference-mediated intrinsic antiviral immunity in plants. Curr. Top. Microbiol. Immunol. 371, 153–181.

Takahashi, T., Zenno, S., Ishibashi, O., Takizawa, T., Saigo, K., Ui-Tei, K., 2014. Interactions between the non-seed region of siRNA and RNA-binding RLC/RISC proteins, Ago and TRBP, in mammalian cells. Nucleic Acids Res. 42 (8), 5256–5269.

Trobaugh, D.W., Gardner, C.L., Sun, C., Haddow, A.D., Wang, E., Chapnik, E., Mildner, A., Weaver, S.C., Ryman, K.D., Klimstra, W.B., 2014. RNA viruses can hijack vertebrate microRNAs to suppress innate immunity. Nature 506 (7487), 245–248.

van Cleef, K.W., van Mierlo, J.T., Miesen, P., Overheul, G.J., Fros, J.J., Schuster, S., Marklewitz, M., Pijlman, G.P., Junglen, S., van Rij, R.P., 2014. Mosquito and Drosophila entomobirnaviruses suppress dsRNA- and siRNA-induced RNAi. Nucleic Acids Res. 42 (13), 8732–8744.

van Mierlo, J.T., Bronkhorst, A.W., Overheul, G.J., Sadanandan, S.A., Ekström, J.O., Heestermans, M., Hultmark, D., Antoniewski, C., van Rij, R.P., 2012. Convergent evolution of argonaute-2 slicer antagonism in two distinct insect RNA viruses. PLoS Pathog. 8 (8), e1002872. http://dx.doi.org/10.1371/journal.ppat.1002872.

van Mierlo, J.T., Overheul, G.J., Obadia, B., van Cleef, K.W., Webster, C.L., Saleh, M.C., Obbard, D.J., van Rij, R.P., 2014. Novel Drosophila viruses encode host-specific suppressors of RNAi. PLoS Pathog. 10 (7), e1004256. http://dx.doi.org/10.1371/journal.ppat.1004256.

van Rij, R.P., Saleh, M.C., Berry, B., Foo, C., Houk, A., Antoniewski, C., Andino, R., 2006. The RNA silencing endonuclease Argonaute 2 mediates specific antiviral immunity in *Drosophila melanogaster*. Genes Dev. 20 (21), 2985–2995.